Linear Stability Analysis of Dispersion-Managed Solitons Controlled by Filters

Junichi Kumasako, Masayuki Matsumoto, *Member, IEEE*, and Suttawassuntorn Waiyapot, *Student Member, IEEE*

***Abstract*—We present a linear stability analysis of dispersion-managed (DM) solitons controlled by inline narrow-band filters. We show that the filters can destabilize the pulse if they are unsuitedly located in the dispersion map, which is contrary to the case of standard solitons in fibers with constant dispersion. We also show that for such an instability to take place the pulse energy and the dispersion-map strength should be significantly larger than those usually required for practical long-distance transmission. The filter-induced instability of DM solitons will be an issue in the operation of stretched-pulse mode-locked fiber lasers.**

***Index Terms*—Fiber ring laser, optical communication, optical soliton, soliton control, stability analysis.**

I. Introduction

ERROR-FREE transmission distances of optical-fiber soliton transmission systems are limited by various perturbations such as nonlinear interaction between adjacent pulses [1], noise-induced timing jitter (Gordon–Haus effect) [2], collision-induced frequency and time shifts in wavelength-division multiplexed systems [3], and so on. Many of these perturbations give shifts in soliton center frequency which are converted to time shifts through fiber dispersion, giving rise to bit errors if the time shifts go beyond acceptance time width at the receiver. Periodic insertion of narrowband filters in the transmission line can reduce the time shifts because the soliton center frequency is attracted to and stabilized at the center frequency of the filter [4], [5]. It is noted that the spectral width of the pulse does not narrowed without limit by the narrowband filter but reaches to a fixed value due to the nonlinear nature of the soliton. If the center frequency of the filter is gradually moved, linear dispersive radiation such as noise coexisting with soliton pulses is attenuated by the filter, which extends the transmission distance further more [6].

These benefits of the filter are mostly kept in dispersion-managed (DM) soliton systems [7]–[9]. When pulse energy is low in a DM system, the spectral width of the pulse is almost constant along the fiber although the temporal width may greatly change in accordance with the periodic change of the fiber dispersion. In this circumstance, the effect of filters on the DM soliton transmission is almost the same as that on standard solitons [7], [8]. When pulse energy is large, however, the spectral width of the pulse changes appreciably in the dispersion-map period and the effect of filters becomes dependent on the filter location in the dispersion map [10]. Furthermore, the dynamics of the pulse under filter control may change qualitatively as the pulse energy, or the strength of DM, grows. It was recently shown that the pulse energy may even be destabilized by the filters [10], [11]. It is interesting to analyze at what pulse energy such instability occurs and how strong the instability is in realistic DM soliton systems.

In this paper we use a linear stability analysis to quantify how bandpass filters can stabilize or destabilize the propagation of DM solitons and examine the dependence of the stability on the location of the filter in the dispersion map [12], [13].

Manuscript received September 23, 1999; revised May 4, 2000.

J. Kumasako was with the Department of Communications Engineering, Osaka University, Osaka 565-0871, Japan. He is now with Fujitsu Laboratories Ltd., Kawasaki, Japan.

M. Matsumoto and S. Waiyapot are with the Department of Communications Engineering, Graduate School of Engineering, Osaka University, Osaka 565-0871, Japan (e-mail: matsumoto@comm.eng.osaka-u.ac.jp).

Publisher Item Identifier S 0733-8724(00)06474-4.

II. Analysis

The analysis is based on coupled nonlinear differential equations for pulse parameters derived by a variational procedure. The equations in an amplifier span $nZ_a < Z < (n+1)Z_a$, where n is an integer and Z_a is the amplifier spacing, are written as [14]

$$\frac{dA}{dZ} = D(Z)AC \tag{1a}$$

$$\frac{d\tau}{dZ} = -2D(Z)\tau C \tag{1b}$$

$$\frac{dC}{dZ} = 2D(Z)C^2 + \frac{1}{2\sqrt{2}}\frac{A^2}{\tau^2}\gamma_{NL}(Z) \cdot \exp\left[-2\int_{nZ_a}^{Z}\Gamma(Z')\,dZ'\right] - \frac{D(Z)}{2\tau^4} \tag{1c}$$

$$\frac{d\kappa}{dZ} = 0. \tag{1d}$$

The above equations are derived by the use of a Gaussian ansats for the pulse

$$q(Z,T) = A\exp[-(T-T_0)^2/(2\tau^2) - i\kappa(T-T_0) - iC(T-T_0)^2 + i\theta]\exp\left[-\int_{nZ_a}^{Z}\Gamma(Z')\,dZ'\right]$$

where A, τ, C, κ, T_0, and θ are amplitude, pulse width, chirp coefficient, frequency, temporal position, and phase of the pulse, respectively, and are functions of the distance. The equations for T_0 and θ are omitted because they are decoupled from the dynamics of the rest of the parameters. Equations (1a)–(1d) correspond to a modified nonlinear Schrödinger equation

$$i\frac{\partial q}{\partial Z} + \frac{D(Z)}{2}\frac{\partial^2 q}{\partial T^2} + \gamma_{NL}(Z)|q|^2 q = -i\Gamma(Z)q \tag{2}$$

where D, γ_{NL}, and Γ are dispersion, nonlinearity, and loss coefficient which may vary with distance. Especially, D alternates

between positive and negative values in DM systems. The amplifier located at $Z = (n+1)Z_a$ amplifies the pulse with a power gain $G = \exp\left[2\int_{nZ_a}^{(n+1)Z_a} \Gamma(Z')\,dZ'\right]$ which compensates for the fiber loss in the amplifier span just before the amplifier.

In the present analysis we assume that a control filter having a Gaussian transfer function of the form $H(\Omega) = \exp(-\beta\Omega^2)$ is inserted in the fiber at every dispersion-map period. $\beta\,(>0)$ is inversely proportional to the square root of the filter bandwidth and represents the strength of the filter. We also assume that the filter is accompanied by an amplitude gain $\exp(\delta)$ which compensates for the energy loss caused by narrowband filtering. Because filters are usually positioned at the amplifier, the gain will be provided by the amplifier as an excess gain. The Gaussian filter transforms the pulse parameters according to

$$A_{\rm out} = \frac{A_{\rm in}}{[(1+2\beta/\tau_{\rm in}^2)^2 + 16\beta C_{\rm in}^2]^{1/4}} \cdot \exp\left[-\frac{\beta\tau_{\rm in}^2\kappa_{\rm in}^2}{\tau_{\rm in}^2 + 2\beta(1+4\tau_{\rm in}^4 C_{\rm in}^2)} + \delta\right] \tag{3a}$$

$$\tau_{\rm out}^2 = \frac{(\tau_{\rm in}^2+2\beta)^2 + 16\beta^2\tau_{\rm in}^4 C_{\rm in}^2}{\tau_{\rm in}^2 + 2\beta(1+4\tau_{\rm in}^4 C_{\rm in}^2)} \tag{3b}$$

$$C_{\rm out} = \frac{\tau_{\rm in}^4 C_{\rm in}}{(\tau_{\rm in}^2+2\beta)^2 + 16\beta^2\tau_{\rm in}^4 C_{\rm in}^2} \tag{3c}$$

$$\kappa_{\rm out} = \frac{\tau_{\rm in}^2\kappa_{\rm in}}{\tau_{\rm in}^2 + 2\beta(1+4\tau_{\rm in}^4 C_{\rm in}^2)} \tag{3d}$$

where the subscripts *in* and *out* indicate quantities at the entrance and the exit of the filter, respectively [15]. Equations (1d) and (3d) determine the dynamics of the frequency κ. Because κ does not change in the fiber as given by (1d) and $0 < \kappa_{\rm out}/\kappa_{\rm in} < 1$ at the filter according to (3d), the frequency is always stabilized at $\kappa = 0$, the center frequency of the filter. It is also found from (3d) that the stabilization of frequency is more efficient when the spectral width of the pulse $\left(\propto\sqrt{1+4\tau^4 C^2}/\tau\right)$ is larger at the filter location.

We now examine the stability of amplitude, temporal width, and chirp after the frequency is stabilized at $\kappa = 0$. We linearize (1a)–(1c) around a stationary DM soliton solution $A_0(Z)$, $\tau_0(Z)$, and $C_0(Z)$ and obtain equations for the evolution of the small deviations ΔA, $\Delta\tau$, and ΔC as follows [12], [13]:

$$\frac{d\Delta A}{dZ} = D(C_0\Delta A + A_0\Delta C) \tag{4a}$$

$$\frac{d\Delta\tau}{dZ} = -2D(C_0\Delta\tau + \tau_0\Delta C) \tag{4b}$$

$$\frac{d\Delta C}{dZ} = 4DC_0\Delta C + \frac{1}{\sqrt{2}}\frac{A_0^2}{\tau_0^2}\left(\frac{\Delta A}{A_0} - \frac{\Delta\tau}{\tau_0}\right)\gamma_{NL} \cdot \exp\left(-2\int_{nZ_a}^{Z}\Gamma\,dZ'\right) + 2D\frac{\Delta\tau}{\tau_0^5}. \tag{4c}$$

We also linearize (3a)–(3c) in terms of the small deviations of the variables (ΔA, $\Delta\tau$, and ΔC), resulting in

$$\Delta A_{\rm out} = K_{11}\Delta A_{\rm in} + K_{12}\Delta\tau_{\rm in} + K_{13}\Delta C_{\rm in} \tag{5a}$$

$$\Delta\tau_{\rm out} = K_{21}\Delta A_{\rm in} + K_{22}\Delta\tau_{\rm in} + K_{23}\Delta C_{\rm in} \tag{5b}$$

$$\Delta C_{\rm out} = K_{31}\Delta A_{\rm in} + K_{32}\Delta\tau_{\rm in} + K_{33}\Delta C_{\rm in}. \tag{5c}$$

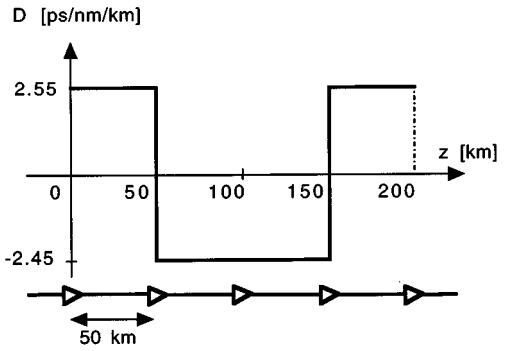

Fig. 1. Dispersion map and amplifier location of a DM system.

Detailed expressions for the coefficients K_{ij} $(i, j = 1 \sim 3)$ are given in Appendix. It is noted that β and δ must satisfy an energy equilibrium condition at the filter

$$\sqrt{(e^{4\delta}-1)/(2\beta)} = \sqrt{1+4\tau_{0,\rm in}^4 C_{0,\rm in}^2}\Big/\tau_{0,\rm in}. \tag{6}$$

Through numerical solution of (4a)–(4c) in a unit cell of the dispersion map together with (5a)–(5c) at the filter, we obtain a 3×3 transfer matrix describing the evolution of the deviations ΔA, $\Delta\tau$, and ΔC in a unit cell. The maximum absolute value of the three eigenvalues λ_i $(i = 1 \sim 3)$ of the matrix determines the stability. We take $P = \max(|\lambda_1|, |\lambda_2|, |\lambda_3|)$ as an index showing the magnitude of the stability. P larger (smaller) than unity indicates that the DM soliton solution is unstable (stable) under the control by the filter.

III. Numerical Examples

As a numerical illustration of the stability analysis, we consider a dispersion map and amplifier arrangement as shown in Fig. 1. The unit cell of the dispersion map consists of anomalous (2.55 ps/nm/km)- and normal (-2.45 ps/nm/km)-dispersion fibers with equal length of 100 km, with which the averaged dispersion is 0.05 ps/nm/km. Four amplifiers are inserted in the unit cell with a spacing of 50 km (they are inserted at $z = 0$, 50, 100, and 150 km in Fig. 1). One of the four amplifiers is accompanied by a narrowband filter. Fiber loss and nonlinearity are 0.2 dB/km and $n_2/A_{\rm eff} = 0.4\times 10^{-9}W^{-1}$, respectively, and are the same for the anomalous- and normal-dispersion fibers.

Fig. 2 shows variations of temporal and spectral widths of the pulse along the fiber of DM soliton solutions having different energies in the absence of filters. These periodic solutions were found by an iterative shooting method applied to the reduced model derived by the variational procedure using Gaussian ansatz. The solutions closely agree with those obtained by the split-step Fourier method. Stability analysis below is made when these DM soliton solutions are attempted to be stabilized by bandpass filters.

Fig. 3 shows the maximum absolute eigenvalue versus the energy (at the output of amplifiers) of the pulse which the filter attempts to stabilize for four different locations of filters. It is found that P is significantly smaller than unity only for the filter location $z_f = 0$ (or 200 km), suggesting that the pulse energy, chirp, and width are effectively stabilized when the filter is located near the middle of the anomalous-dispersion fiber section.

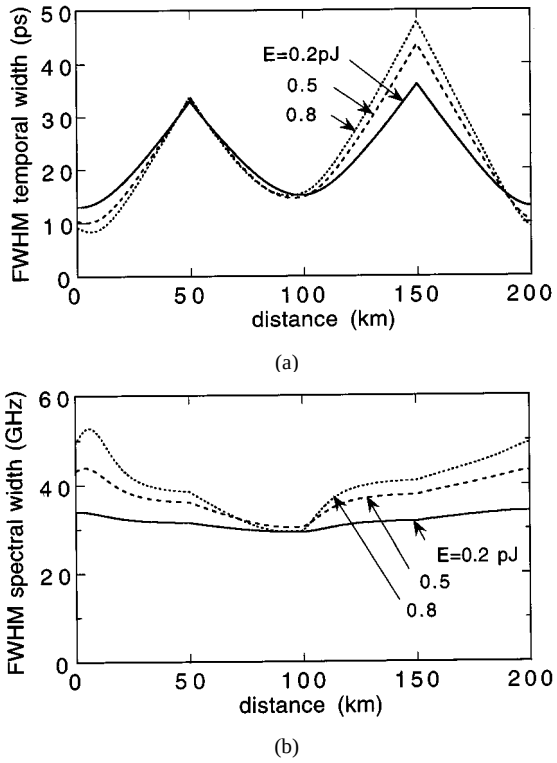

Fig. 2. (a) Temporal width and (b) spectral width of the DM soliton solution versus distance along the fiber in a unit cell of the dispersion map. Pulse energies at the amplifier output are 0.2, 0.5, and 0.8 pJ. No filters are inserted.

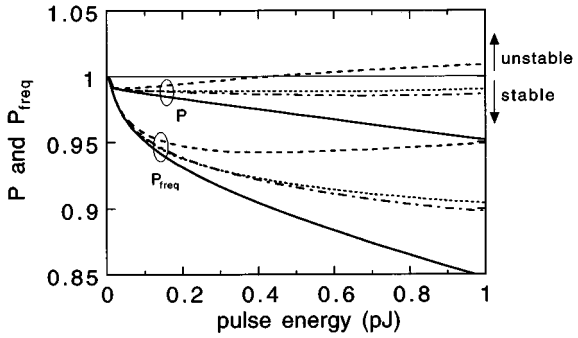

Fig. 3. Maximum absolute eigenvalue $P = \max(|\lambda_1|, |\lambda_2|, |\lambda_3|)$ of the transfer matrix for ΔA, $\Delta\tau$, and ΔC versus the pulse energy. Filter locations are $z_f = 0$ km (solid curve), 50 km (dotted curve), 100 km (dashed curve), or 150 km (dash-dotted curve). Frequency stabilization coefficient $P_{\rm freq}$ for these filter locations is also shown.

When filters are placed at other amplifier locations, P remains close to unity and even becomes larger than unity for $z_f = 100$ km, indicating that the energy, chirp, and width of the pulse may be destabilized by the filters. This is qualitatively understood by the spectral behavior of the DM soliton solution: spectral width of the pulse becomes decreasing function of the pulse energy at $z = 100$ km in Fig. 1 when the energy is sufficiently large as shown in Fig. 4. When enhanced pulse energy leads to decreased spectral width, the bandpass filter acts on the pulse to destabilize its energy [10]. The accurate stability, however, can not be predicted by the relation between the spectral width and energy in the steady state. The relation only describes slow adiabatic dynamical behavior of the pulse energy. When the strength of

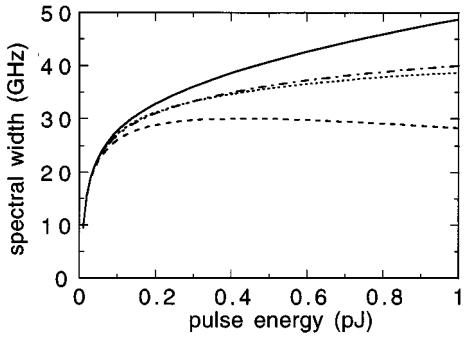

Fig. 4. Spectral width at $z = 0$ km (solid curve), 50 km (dotted curve), 100 km (dashed curve), and 150 km (dash-dotted curve) versus pulse energy of a DM soliton solution.

the filter is not very small, we need to use analysis as given in the previous section. In Fig. 3, we also plot the frequency stabilization coefficient

$$P_{\rm freq} = \tau_{0,\,\rm in}^2/[\tau_{0,\,\rm in}^2 + 2\beta(1 + 4\tau_{0,\,\rm in}^4 C_{0,\,\rm in}^2)] \qquad (7)$$

see (3d). It is shown that weaker stabilization of the amplitude accompanies weaker stabilization of the frequency.

In Figs. 5 and 6, we show actual evolution of pulse energy obtained either by the variational analysis based on (1) and (3) or by the numerical solution of (2) with using the Gaussian spectral response for the filter. In each of Figs. 5 and 6, filters having 3 dB bandwidth of 1.0 nm are located at (a): $z_f = 0$ or (b) $z_f = 100$ km. The excess gain δ is chosen so that the relation (6) is satisfied for respective filter location and equilibrium pulse energy. The excess gain is adjusted slightly (within 0.2%) in the numerical solution so that the steady-state pulse energy becomes roughly the same for the variational and numerical analyses. Fig. 5(a) and (b) are the results when a pulse with energy $E_p = 0.2$ pJ is stabilized. The initial pulse at $z = 0$ is Gaussian with $(A(0)\,\tau(0),\, C(0)) = (A_*,\, \tau_*,\, C_*)$, $(1.01A_*,\, 1.01\tau_*,\, C_*)$, or $(0.99A_*,\, 0.99\tau_*,\, C_*)$, where A_*, τ_*, and C_* are those of the DM soliton solution in the presence of filters with $E_p = 0.2$ pJ. The pulse energy is attracted to a fixed value in both Fig. 5(a) and (b), with stronger stabilization in Fig. 5(a) than in Fig. 5(b), which agrees with the preceding stability analysis. It is also shown that the variational and numerical results agree well. Fig. 6(a) and (b) are the results when a pulse with energy $E_p = 0.8$ pJ is attempted to be stabilized. When the filter location is $Z_f = 100$ km [Fig. 6(b)], the pulse energy is not stabilized at a fixed value, which agrees with the result of the stability analysis where P is larger than unity when $z_f = 100$ km and $E_p \gtrsim 0.45$ pJ.

In the numerical example the filter bandwidth is fixed at 1.0 nm. Qualitatively the same dynamical pulse behavior is obtained with shorter distance scale for narrower filter bandwidths. In this case, however, another kind of instability caused by the growth of background radiation appears at relatively short transmission distances. The background instability can be avoided by sliding the center frequency of the filter, which enables us to use strong filters. Filter-induced instability analyzed here will be more important for such circumstances.

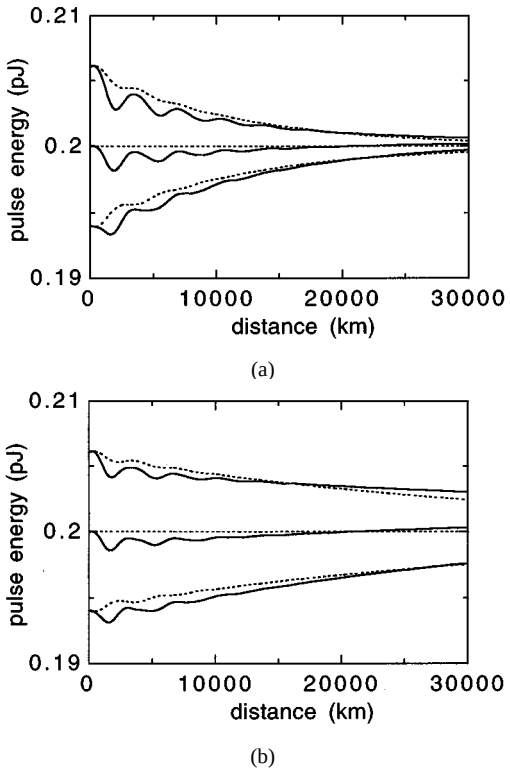

Fig. 5. Evolution of pulse energy when a Gaussian filter with 1-nm bandwidth is inserted at: (a) $z = 0$ and (b) $z = 100$ km. Solid and dotted curves are obtained by the split-step Fourier numerical method and by the variational method, respectively. The excess gain δ is chosen so that the pulse energy is to be stabilized at $E_p = 0.2$ pJ.

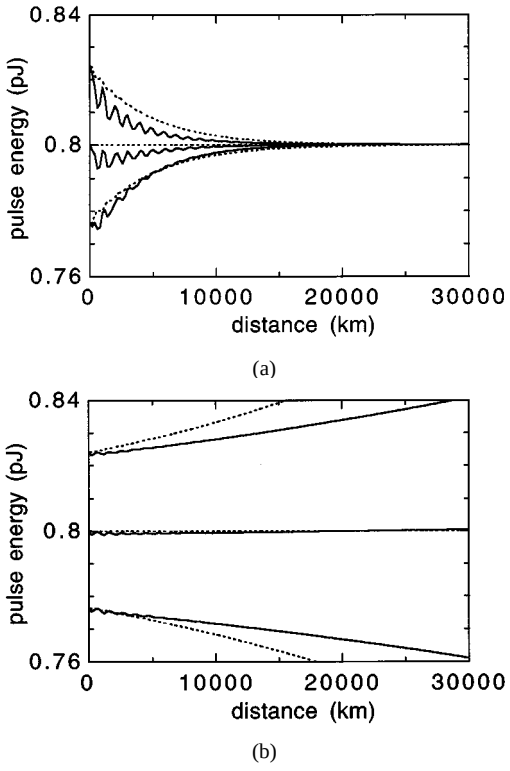

Fig. 6. Evolution of pulse energy when a Gaussian filter with 1-nm bandwidth is inserted at: (a) $z = 0$ and (b) $z = 100$ km. Solid and dotted curves are obtained by the split-step Fourier numerical method and by the variational method, respectively. The excess gain δ is chosen so that the pulse energy is to be stabilized at $E_p = 0.8$ pJ.

It is noted here that although the filter-induced instability is harmful in general to achieve stable long-distance pulse transmission, it may be advantageously utilized in some applications where analog information is sent by the modulation of pulse amplitudes. Such applications include passive loop-back line monitoring where low-index and low-frequency modulations are imposed on the pulse train to monitor the status of individual in-line amplifiers in a long-distance transmission line [16].

IV. Discussion

The results given in the previous section indicate that the pulse energy should be larger than about 0.5 pJ for the filter-induced instability to appear in the dispersion map shown in Fig. 1. The pulse energy is far larger than that required to achieve error-free transmission in long-distance amplified systems. The Q factor, an equivalent of the electrical SN ratio at the receiver, is given as a function of pulse energy as [17]

$$Q = \frac{E_p R}{\sqrt{2NE_pR^2 + MBN^2R} + \sqrt{MBN^2R}} \tag{8}$$

where E_p, R, N, B, M are pulse energy, bit rate, power spectral density of ASE noise ($= Khvn_{sp}(G-1)$, where K, hv, and n_{sp} are the number of amplifiers inserted in the system, photon energy, and spontaneous emission factor of the amplifier), bandwidth of the optical filter prior to photodetection, and the number of detected optical modes, respectively. In the expression (8) signal–ASE and ASE–ASE beat noise contributions are taken into account. When $K = 180$, which assumes 9000 km distance with amplifier spacing 50 km, $n_{sp} = 2$, $G = 11$ dB, $B = 2R$, and $M = 2$ (unpolarized detection), $E_p \gtrsim 0.06$ pJ gives rise to $Q > 6$, or BER $< 10^{-9}$. Thus the pulse energy with which the filter-induced instability may occur is larger about by an order of magnitude than that required for negligible bit error in terms of the signal-to-noise ratio (SNR).

According to an analysis under the lossless assumption, the filter-induced instability arises when an inequality $l\Delta\beta''/t_{\mathrm{FWHM}}^2$ (dispersion-map strength) $\gtrsim 4$ for a symmetrical dispersion map with $\beta''_{\mathrm{ave}}/\Delta\beta'' = 0.04$, where l, $\Delta\beta''$, β''_{ave}, and t_{FWHM} are half the dispersion-map period, difference of the group-velocity dispersions (GVD) of normal and anomalous dispersion fibers, averaged GVD, and FWHM pulse width at the midpoint of the anomalous-dispersion fiber, respectively [10]. According to this inequality the filter-induced instability may take place at lower pulse energies when the absolute value of the fiber dispersion is lowered while the dispersion-map period is increased with their product kept constant. However, such a dispersion profile is impractical and, even if it is used, very long transmission distance will be needed for the unstable dynamics of the pulse to be observed. Moreover the interaction between adjacent pulses will limit the error-free transmission distance for such a large dispersion-map strength.

The filter-induced instability in DM soliton propagation does, therefore, not seem to become a serious issue in long-distance transmission systems. The soliton propagation in an optical fiber

with alternating sign of GVD, on the other hand, is the basis of the operation of stretched-pulse mode-locked fiber lasers, from which high-energy subpicosecond pulses can be produced [18]. Since such lasers are usually operated with large dispersion-map strength and large pulse separation, the filter-induced instability discussed in this paper is expected to appear. Careful consideration on the filter location will be needed for stable operation of such lasers when filters are incorporated in the cavity.

V. Conclusion

We presented a linear stability analysis of DM solitons controlled by bandpass filters. The analysis can show how the filters can stabilize (or destabilize) the frequency and energy of the DM soliton depending on their position in the dispersion map. The destabilization of the pulse may arise when the filter is located near the midpoint of the anomalous-dispersion fiber section. It was shown, however, that for such instability to take place the pulse energy and the dispersion-map strength should be significantly larger than those required for practical long-distance transmission. The filter-induced instability of DM solitons will be more pertinent in the operation of the stretched-pulse mode-locked fiber laser, pulse dynamics in which is similar to that in long-distance transmission but usually operated with large pulse energy and small duty ratio.

Appendix

Coefficients appearing in (5a)–(5c) are given as follows:

$$
\begin{aligned}
K_{11} &= e^{\delta} F_1^{-1/4}, \\
K_{12} &= 2e^{\delta}\beta F_1^{-5/4} A_{0,\mathrm{in}}(2\beta + \tau_{0,\mathrm{in}}^2)/\tau_{0,\mathrm{in}}^5, \\
K_{13} &= -8e^{\delta}\beta^2 F_1^{-5/4} A_{0,\mathrm{in}} C_{0,\mathrm{in}}, \\
K_{21} &= 0, \\
K_{22} &= F_2 \tau_{0,\mathrm{in}}/(F_3^{3/2} F_4^{1/2}), \\
K_{23} &= -8\beta(2\beta + \tau_{0,\mathrm{in}}^2)\tau_{0,\mathrm{in}}^6 C_{0,\mathrm{in}}/(F_3^{3/2} F_4^{1/2}), \\
K_{31} &= 0, \\
K_{32} &= 8\beta(2\beta + \tau_{0,\mathrm{in}}^2)\tau_{0,\mathrm{in}}^3 C_{0,\mathrm{in}}/F_4^2, \\
K_{33} &= F_2 \tau_{0,\mathrm{in}}^4/F_4^2
\end{aligned}
$$

where F_i ($i = 1 \sim 4$) are

$$
\begin{aligned}
F_1 &= (1 + 2\beta/\tau_{0,\mathrm{in}}^2)^2 + 16\beta^2 C_{0,\mathrm{in}}^2, \\
F_2 &= (2\beta + \tau_{0,\mathrm{in}}^2)^2 - 16\beta^2 \tau_{0,\mathrm{in}}^4 C_{0,\mathrm{in}}^2, \\
F_3 &= \tau_{0,\mathrm{in}}^2 + 2\beta(1 + 4\tau_{0,\mathrm{in}}^4 C_{0,\mathrm{in}}^2), \\
F_4 &= (2\beta + \tau_{0,\mathrm{in}}^2)^2 + 16\beta^2 \tau_{0,\mathrm{in}}^4 C_{0,\mathrm{in}}^2.
\end{aligned}
$$

The subscript 0, in indicates that the quantity is that of the stationary solution at the entrance of the filter.

References

[1] J. P. Gordon, "Interaction forces among solitons in optical fibers," *Opt. Lett.*, vol. 8, pp. 596–598, 1983.

[2] J. P. Gordon and H. A. Haus, "Random walk of coherently amplified solitons in optical fiber transmission," *Opt. Lett.*, vol. 11, pp. 665–667, 1986.

[3] L. F. Mollenauer, S. G. Evangelides, and J. P. Gordon, "Wavelength division multiplexing with solitons in ultra-long distance transmission using lumped amplifiers," *J. Lightwave Technol.*, vol. 9, pp. 362–367, 1991.

[4] A. Mecozzi, J. D. Moores, H. A. Haus, and Y. Lai, "Soliton transmission control," *Opt. Lett.*, vol. 16, pp. 1841–1843, 1991.

[5] Y. Kodama and A. Hasegawa, "Generation of asymptotically stable optical solitons and suppression of the Gordon–Haus effect," *Opt. Lett.*, vol. 17, pp. 31–33, 1992.

[6] L. F. Mollenauer, J. P. Gordon, and S. G. Evangelides, "The sliding-frequency guiding filter: An improved form of soliton jitter control," *Opt. Lett.*, vol. 17, pp. 1575–1577, 1992.

[7] E. A. Golovchenko, J. M. Jacob, A. N. Pilipetskii, C. R. Menyuk, and G. M. Carter, "Dispersion-managed solitons in a fiber loop with in-line filtering," *Opt. Lett.*, vol. 22, pp. 289–291, 1997.

[8] G. M. Carter and J. M. Jacob, "Dynamics of solitons in filtered dispersion-managed systems," *IEEE Photon. Technol. Lett.*, vol. 10, pp. 546–548, 1998.

[9] M. Matsumoto, "Analysis of filter control of dispersion-managed soliton transmission," *J. Opt. Soc. Amer. B*, vol. 15, pp. 2831–2837, 1998.

[10] ——, "Instability of dispersion-managed solitons in a system with filtering," *Opt. Lett.*, vol. 23, pp. 1901–1903, 1998.

[11] F. Merlaud and T. Georges, "Influence of filtering on jitter and amplitude fluctuations for dispersion managed solitons," in *Proc. 24th Eur. Conf. Optical Commun.*, 1998, Paper WdB22, pp. 497–498.

[12] M. Matsumoto and S. Waiyapot, "Linear stability analysis of dispersion-managed solitons controlled by filters," in *Proc. Conf. Lasers and Electro-Optics, OSA Tech. Dig.*. Washington, DC: Optical Society of America, 1999, p. 234.

[13] S. Waiyapot and M. Matsumoto, "Stability analysis of dispersion-managed solitons controlled by synchronous amplitude modulators," *IEEE Photon. Technol. Lett.*, vol. 11, Nov. 1999.

[14] M. Matsumoto and H. A. Haus, "Stretched-pulse optical fiber communications," *IEEE Photon. Technol. Lett.*, vol. 9, pp. 785–787, 1997.

[15] M. Matsumoto, "Effects of guiding filters on stretched-pulse transmission in dispersion-managed fibres," *Electron. Lett.*, vol. 33, pp. 1718–1720, 1997.

[16] M. Matsumoto and H. A. Haus, "Transmission of line-monitoring signals in stretched-pulse communication systems," in *Proc. 23rd Eur. Conf. Optical Commun.*, 1997, IEE Conf. Publ. 448, pp. 267–270.

[17] O. K. Tonguz, "Impact of spontaneous emission noise on the sensitivity of direct-detection lightwave receivers using optical amplifiers," *Electron. Lett.*, vol. 26, pp. 1343–1344, 1990.

[18] H. A. Haus, K. Tamura, L. E. Nelson, and E. P. Ippen, "Stretched-pulse additive pulse mode-locking in fiber ring lasers: Theory and experiment," *IEEE J. Quantum Electron.*, vol. 31, pp. 591–598, 1995.

Junichi Kumasako as born in Shiga, Japan, on February 26, 1974. He received the B.S. and M.S. degrees in communication engineering from Osaka University, Osaka, Japan, in 1997 and 1999, respectively.

He is currently working at Fujitsu Laboratories Ltd., Kawasaki, Japan.

Mr. Kumasako is a member of the Institute of Electronics, Information and Communication Engineers (IEICE) of Japan.

Masayuki Matsumoto (M'85) was born in Osaka, Japan, in 1960. He received the B.S., M.S., and Ph.D. degrees in engineering from Osaka University, Suita, Osaka, Japan, in 1982, 1984, and 1988, respectively.

Since 1985, he has been with the Department of Communication Engineering, Osaka University, where he is now an Associate Professor. His present research interests are in the areas of optical fiber communications and nonlinear fiber optics, especially, soliton transmission in fibers.

Dr. Matsumoto is a member of the Optical Society of America (OSA) and the Institute of Electronics, Information and Communication Engineers (IEICE) of Japan.

Suttawassuntorn Waiyapot (S'99) was born in Chiangrai, Thailand. He received the B.E. degree in electrical engineering from Chulalongkorn University, Thailand, in 1995 and M.E. degree in electrical and electronic engineering from Miyazaki University, Japan, in 1998. He is currently working toward the Ph.D. degree in communication engineering at Osaka University, Japan.

His research interests are in the areas of optical soliton transmission and fiber ring laser.